ANALYTICAL BIOCHEMISTRY 196, 326–336 (1991)

Modeling of Immunosensors under Nonequilibrium Conditions

II. Experimental Determination of Performance Characteristics[1]

Willfried Schramm*,† and Se-Hwan Paek*

*The University of Michigan, Reproductive Sciences Program and Bioengineering Program, 300 North Ingalls, Ann Arbor, Michigan 48109; and †BioQuant, Inc., 1919 Green Road, Ann Arbor, Michigan 48105

Received December 17, 1990

In an attempt to optimize immunosensors operating with an immobilized antibody as binding protein and an analyte–enzyme conjugate as signal generator that is significantly larger in molecular size than the analyte, in a previous communication (Part I) (S.-H. Paek and W. Schramm (1991) *Anal. Biochem.* 196) we developed mathematical models for the prediction of performance characteristics. These models are compared in this contribution with experimentally obtained results. As an example, a monoclonal antibody to the steroid hormone progesterone has been used as binding protein, an ^{125}I-progesterone derivative, and a progesterone–horseradish peroxidase derivative as tracers for signal generation. A minimum of parameters needs to be experimentally determined to calculate the performance: the amount of immobilized antibody, the diffusion coefficient of antigens, the thickness of the penetration layer, and the on- and off-rates for binding of the antigen to the antibody. We have described simple methods to obtain these data for the labeled antigen and for the unlabeled analyte that does not provide a signal per se. Kinetic binding curves for antigen–antibody complex formation obtained with the mathematical models correlated well with experimentally obtained results for antigens of different sizes. Although equilibrium of the antigen–antibody complex for the enzyme-labeled analyte conjugate requires about 4 h in the absence of free analyte, dose–response curves can be obtained after 5 min and the relative position of these curves does not change significantly after 30 min. Using a total volume of 200 μl for the analytical procedure in microtiter wells, agitation as a means to accelerate convective diffusion during an incubation period of 30 min is not necessary with the analyte–enzyme conjugate. However, immunosensors using large analyte–enzyme conjugates as signal generators for the detection of small analytes require strict control of the incubation time if operated within short periods of time (<30 min).

In a previous communication (Part I) (1), we have investigated mathematical models for the prediction of performance characteristics of immunosensors for small analytes with immobilized antibodies as specific binding proteins. If small analytes are detected by means of large analyte–enzyme complexes as signal generators, the formation rate of an encounter complex between an immobilized immunoglobulin and an antigen (i.e., the precursor for the antigen–antibody complex) is determined by the different diffusion rates of the antigens of different size. The diffusion processes involved have been analyzed and equations for the calculation of the major components contributing to diffusion have been given. In addition, for the calculation of time-variable concentrations of antigens bound to the immobilized antibody (kinetic binding curves), we have provided equations for two mathematical approaches: an analytical solution and a numerical solution. In this paper (Part II), we compare experimentally obtained results with the theoretical calculations.

By way of example, we have carried out the experiments in microwells which we have also selected as the basis for our calculations in Part I. All the symbols used in this paper refer to Table I in Part I. The models that we have described have general application for engineering sensors that are used for the detection of small analytes by means of a large analyte–enzyme conjugate in competitive immunoassays. However, microwells are convenient carriers for the preliminary selection of op-

[1] Part I: Mathematic modeling of performance characteristics.

0003-2697/91 $3.00

timal reagents and conditions before proceeding to more complex systems. We are using the methods described in this paper for the development of electrodes with amperometric signal detection. The results of that project will be the subject of a later communication.

MATERIALS AND METHODS

Materials

Horseradish peroxidase (HRP,[2] type VI, 300 units/mg solid; EC 1.11.1.7), 1,5-diaminopentane (cadaverine), poly-L-lysine hydrobromide (M_r 421,000 by viscosity test), and 3,3',5,5'-tetramethylbenzidine (TMB) were purchased from Sigma (St. Louis, MO). Disuccinimidyl suberate (DSS), CNBr-activated Sepharose 4B, Bio-Gel P-30, and Immulon II microtiter wells were obtained from Pierce (Rockford, IL), Pharmacia Fine Chemicals, Inc. (Piscataway, NJ), Bio-Rad (Richmond, CA), and Dynatech Inc. (Alexandria, VA), respectively. The following monoclonal antibodies were produced in this laboratory (2): two antibodies to progesterone (P-Ab), one with a high affinity constant (BQ.1) and the other with a low affinity constant (4C10); and an antibody to urease (NS-Ab).

Progesterone derivatives. Progesterone derivatives were synthesized and characterized by HPLC (2): progesterone-11α-*N*-hydroxy succinimide (P-NHS), progesterone-11α-hemisuccinyl-1,5-diaminopentane (P-CAD) by reacting P-NHS with cadaverine, and progesterone-11α-hemisuccinyl tyrosine methyl ester (P-TME). The P-TME was iodinated (^{125}I-P) with the carrier-free [^{125}I] (NEN Research Products, DuPont Co., Wilmington, DE), purified, and characterized according to the methods as described (2).

Substrate for HRP. The substrate solution for HRP contained 10μl of 3% (v/v) H_2O_2 in water, 100 μl of 10 mg/ml TMB in dimethyl sulfoxide, and 10 ml of 50 mM acetate buffer, pH 5.1.

Immobilization of Antibody to Microtiter Wells

Two monoclonal antibodies were immobilized on the surface of microtiter wells: P-Ab (BQ.1) and NS-Ab. The immobilization was accomplished by a modified procedure of the sodium periodate method (3). The microwell surface was treated by 200 μl of 10 μg/ml poly-L-lysine in 0.5 M carbonate buffer, pH 9.6; the lysine was reacted with antibody (2.5 or 5 μg/ml) activated by 0.3 mM $NaIO_4$, and the resulting imide bonds were stabilized with 1 mM $NaCNBH_3$ in 10 mM phosphate buffer, pH 7.0, containing 140 mM NaCl and 0.02% (w/v) thimerosal (Buffer A) and 0.1% (w/v) gelatin (Buffer B). The treated wells were dried under vacuum and stored in the presence of silica gel as desiccant at 4°C.

Preparation of a Defined Progesterone–HRP Conjugate

The progesterone derivative, P-CAD, was chemically reacted with the enzyme, HRP, via DSS as a cross-linking reagent. The conjugates were synthesized by: (a) reacting P-CAD with 2 molar excess of cross-linking reagent, (b) after incubation for 30 min on a shaker, adding this mixture to enzyme with 20 molar excess of P-CAD, and (c) incubation for 2 h on a shaker. The reaction mixture of progesterone–HRP conjugate was dialyzed in Buffer A, and then partially purified by exclusion chromatography on Bio-Gel P-30.

The conjugation mixture was finally purified on an immunoaffinity column (1.1 × 37 cm, 20 ml bed vol) with the IgG to progesterone, 4C10, immobilized on CNBr-activated Sepharose 4B gel. The purified conjugate with one progesterone molecule bound to one HRP molecule (P-HRP) was selected, diluted with the same volume of Buffer B, and stored at −4°C. The concentration of P-HRP in solution was determined by comparing its activity in a solid-phase assay with standard concentrations of free HRP. The enzymatic activity of the conjugate was preserved without loss for more than 1 year.

Determination of Parameters for Labeled Antigens

For quantitative estimations, we considered for the microwells a cylindrical geometry with 6.4-mm diameter and 6.2-mm height for a fill volume of 200 μl per well.

If not otherwise mentioned, all assays were performed in duplicate, and the means were used for the plots. The microwells with immobilized P-Ab used for the determination of parameters were prepared by incubating 200 μl of 5 μg/ml BQ.1. Nonspecific binding measured by NS-Ab was subtracted from total binding.

Surface density of antibodies on solid surfaces. The labeled progesterone (e.g., P-HRP, ^{125}I-P) was incubated at different concentrations in microwells that contained P-Ab. The buffer used for the dilution of the antigens was Buffer B unless otherwise mentioned. After incubating 2 h for small antigens (e.g., native progesterone, ^{125}I-P) or 5 h for a large antigen (e.g., P-HRP), the unbound portion was separated by washing the microwells with deionized water. The concentration of bound antigen was determined by colorimetric detection for the enzyme conjugate or by monitoring the γ-ra-

[2] Abbreviations used: HRP, horseradish peroxidase; TMB, 3,3',5,5'-tetramethylbenzidine; DSS, disuccinimidyl suberate; P-Ab, monoclonal antibody specific to progesterone; NS-Ab, monoclonal antibody specific to urease, i.e., nonspecific antibody to progesterone; P-NHS, progesterone-11α-*N*-hydroxy succinimide; P-CAD, progesterone-11α-hemisuccinyl-1,5-diaminopentane; P-TME, progesterone-11α-hemisuccinyltyrosine methyl ester; ^{125}I-P, ^{125}I-labeled progesterone; P-HRP, HRP with one progesterone ligand per enzyme molecule.

diation of the radiolabeled derivative with a γ-counter. The concentration of antibody measured by each labeled antigen were determined by Scatchard analysis (4).

On-rate constants. The on-rate constant of the P-HRP to P-Ab was measured by incubating 200 μl of the labeled analyte (45 pM P-HRP or 64 pM ^{125}I-P) in the microwells with the immobilized antibody for different time intervals. The microwells were agitated on a shaker to facilitate mass transfer of the antigen from the bulk solution to the solid surface. At predetermined times, the unbound antigen was separated, and the concentration of the bound antigen was measured as described above.

Off-rate constants. To measure the dissociation rate constant of P-HRP from the antigen–antibody complex, 200 μl of the labeled analyte (120 pM P-HRP or 2.8 nM ^{125}I-P) was preincubated in the wells with the immobilized antibody. After incubating for 2 to 5 h, the wells were washed, and 200 μl of about 300 nM P-Ab was added to capture dissociating antigen. At predetermined time intervals, the wells were washed and the concentrations of the bound antigen were measured. These experiments were also carried out with agitation (stirring conditions).

Effective diffusion coefficients. The effective diffusion coefficients were determined for P-HRP and for ^{125}I-P. The experimental setup was identical to that used for the determination of the on-rate constants except that nonstirring conditions were used.

Penetration (hydrodynamic) layer thickness. The thickness of the layer on the solid surface that was not disturbed by agitation (penetration layer) was derived from the initial binding rates of radiolabeled and enzyme-labeled tracers as described under Results and Discussion. To determine the initial binding rates, we incubated in P-Ab-coated wells 190 μl of Buffer B and 10 μl of the labeled analyte (0.9 n*M* P-HRP or 1.3 n*M* ^{125}I-P) under agitation on an orbital shaker. The amount of labeled antigen bound after 10, 20, and 30 s was determined.

Determination of Parameters for Native Antigen

Contrary to labeled antigens, the native antigen does not generate signals that are readily measurable. Therefore, the four variables described above were obtained by indirect methods. The on/off-rate constants were measured for the native antigen while the antibody concentration on the solid surface and the effective diffusion coefficient were substituted with results obtained with ^{125}I-P as tracer.

The methods used for the determination of the on/off-rate constants of the native antigen were as follows: (a) determine the equilibrium binding constant (5) from dose–response curves (see below) by using ^{125}I-P as signal generator, (b) measure indirectly the off-rate constant by means of ^{125}I-P, and (c) calculate the on-rate constant from the determined two values.

Off-rate constant. Two hundred microliters of 320 nM progesterone was incubated in the microwells with the immobilized antibody. After incubation for 2 h, unbound antigen was separated, and 200 μl of 2.8 nM ^{125}I-P was added to the wells. At predetermined times, the wells were washed, and the remaining radioactivities were measured. The measured concentration of the bound radiolabeled analyte indicated the amount of the dissociated native analyte from the binding complex with the antibody (for details see below).

Kinetic Binding Curves

The kinetic binding curves of antigens to antibody were obtained by measuring the concentrations of the bound antigen over time as described for the determination of the penetration layer thickness except for the incubation periods (binding of analytes was followed for up to 5 h).

Dose–response Curves

Dose–response curves were obtained by a competitive immunoassay in microwells with immobilized antibody (coat with 200 μl of 2.5 μg/ml of BQ.1) and labeled progesterone as tracer (i.e., P-HRP or ^{125}I-P) under nonequilibrium and equilibrium conditions. Equilibrium of the antigen–antibody complex formation was determined by measurement of labeled antigen over time. A solution with a constant concentration of the labeled antigen (50 μl of 350 pM P-HRP, 50 μl of 300 pM) and different concentrations of progesterone in Buffer B was added to the wells (total volume 200 μl), and incubated for 2 h (radiolabeled tracer) and 5 h (enzyme labeled tracer) on an orbital shaker, after which equilibrium with the respective tracers was reached. After washing the wells, the signal from the bound labeled progesterone was measured as described above. The dose–respone curves were analyzed by the log–logit transformation (6).

RESULTS AND DISCUSSION

Empirical Determination of Parameters

To calculate the concentrations of antigen bound to the antibody over time by means of the analytical and numerical solution (Part I), we need to determine experimentally the following values: (a) surface density of antibodies on the solid matrix, (b) on/off-rate constants, (c) effective diffusion coefficients, and (d) penetration layer thickness. For immunosensors that use la-

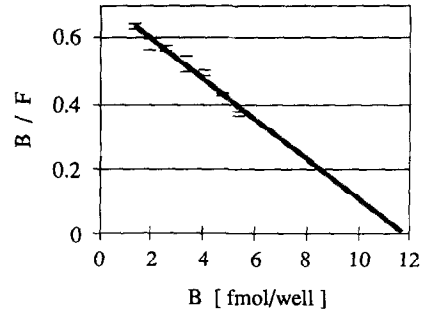

FIG. 1. *Scatchard representation of binding of enzyme-labeled antigen to immobilized antibody.* The affinity constant K_a was calculated from the slope of the regression line and the number of binding sites on the solid surface from the intercept on the x-axis ($K_a = 1.2 \times 10^{10}$ liter/mol). The variation of B/F for duplicate determinations are shown.

beled and nonlabeled antigens, the on/off-rate constants and diffusion coefficients for these species need to be separately determined. As mentioned previously, this might not be straightforward for the native antigen which usually does not provide a physically measurable signal.

For the purpose of this study, we have selected a solid-phase assay using an immobilized monoclonal antibody to the steroid hormone progesterone (2,7) and with a progesterone–horseradish peroxidase conjugate as signal generator (tracer). For comparisons, we have also used a ^{125}I-tyrosine methyl ester bound to progesterone as tracer.

Determination of Independent Variables for Labeled Antigens

In the following examples, we demonstrate the empirical determinations of variables by means of a conjugate between progesterone and horseradish peroxidase which was purified by affinity chromatography. The antigen–antibody complex with this conjugate was measured by a colorimetric reaction with tetramethylbenzidine (8).

Surface density of antibodies (T'). To determine the amount of antibody (T') on the surface of microwells, the ratio of the bound conjugate (B) to the unbound (F) is plotted against B (Fig. 1) according to the Scatchard equation (3),

$$B/F = K_a T' - K_a B, \qquad [1]$$

where K_a is the equilibrium binding constant. Plotting B/F vs B provided a straight line for linear regression which indicates that a homogeneous population of antigen–antibody complex is present. The slope of the regression line allows one to determine K_a. The concentration of antibody T' can then be extrapolated from the x-intercept. Calculated T' in this example is expressed as moles per well. For the computations of the equations presented in Part I, we have converted moles per well into moles per mm^2.

The determination of the maximal number of binding sites for analyte–enzyme conjugates by methods that require extrapolation may meet some technical limitations. For example, in the Scatchard plot (Fig. 1), values close to zero B/F are impossible to obtain because a large concentration of bound enzyme conjugate develops colored products so fast that linear measurement of the optical density becomes a problem. Therefore, one needs to extrapolate the regression line over some distance which may lead to some inaccuracy in the number of binding sites, B. Despite the large extrapolation in this example, we obtained good agreement between the model and experimental results.

On-rate constant (k_{on}). The rate equation for the antigen–antibody binding (Part I) is simplified by neglecting the off-rate (dissociation), and the concentration of unoccupied binding sites is substituted with the concentrations of total and occupied binding sites from the law of mass action for the antibody. After integration, the following simple expression [2] for the empirical determination of the on-rate constant is obtained (9),

$$-\ln\{(T - B)/(T' - B)\} = -(T - T')k_{on}t + \ln(T'/T), \qquad [2]$$

where T is total concentration of antigen per well. The on-rate constant, k_{on}, can be calculated from the slope $(-(T - T')k_{on})$ of the plot $(-\ln\{(T - B)/(T' - B)\})$ vs t. However, experimental results of the plot (Fig. 2) are nonlinear for two reasons: (a) the binding reaction becomes diffusion limited, i.e., the on-reaction rate exceeds the diffusion rate of the molecules to the immobi-

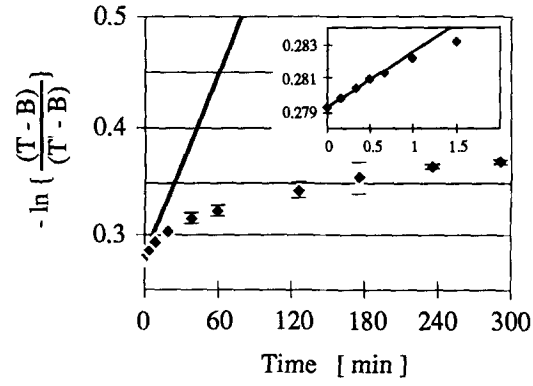

FIG. 2. Determination of the on-rate constant, k_{on}, for binding of progesterone–HRP conjugate to immobilized antibody over time. From the initial data, a linear regression line is constructed (Inset). The slope can be used to calculate k_{on}.

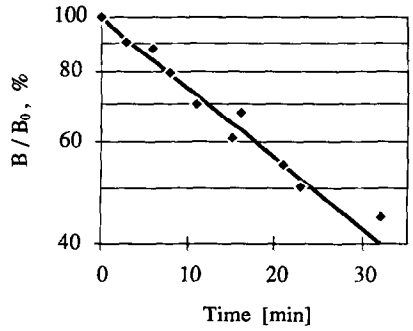

FIG. 3. Determination of the off-rate constant, k_{off}. The dissociation of progesterone-HRP conjugate from immobilized antibody is measured over time. A linear regression line is constructed from the remaining bound conjugate before reassociation superimposes dissociation. The slope represents k_{off}.

lized antibody, and (b) dissociation supersedes association increasingly with time. However, both factors are negligible at the initial period of the reaction. The on-rate is determined by measuring the initial slope for binding of the antigen (10) before the reaction is diffusion controlled. Therefore, the slope is typically measured within the first 30 s.

Off-rate constant (k_{off}). The dissociation rate of the antigen from the antigen–antibody complex on the solid surface was measured in the presence of excess antibody in solution to capture the dissociating antigen. We used an antibody concentration of 300 nM that provided a mean free path between the antibody molecules in solution of 2×10^{-3} mm which is 45 times shorter than the penetration layer thickness (9×10^{-2} mm). The antibody concentration is sufficiently high so that antigen dissociation is not diffusion controlled at the initial period. Under this condition, the on-rate term in the reaction rate equation can be neglected and we obtain [3] after integration,

$$\log(B/B_0) = -k_{off}t/2.303, \qquad [3]$$

where B_0 is the concentration of the binding complex at the initial time. As shown in Fig. 3, the plot of experimental data of $[\log(B/B_0)]$ vs t follows initially a linear regression with the slope of $(-k_{off}/2.303)$. However, at extended periods of incubation, reassociation of the dissociated antigen accounts for deviation from linearity. Therefore, the slope is constructed only from the data obtained from the initial incubation period (20 min). This method gives an approximation for k_{off} by using the linear range of the curve before reassociation starts to affect the equilibrium (10).

Effective diffusion coefficient (D). Under nonstirring conditions, the antigen–antibody complex formation might be diffusion controlled. In that case, it is assumed that the amount of antigen bound to antibody will be equal to the amount of antigen that reaches the surface by diffusion. The relation between bound antigen and the diffusion rate is shown in Eq. [4] for planar surfaces. This equation can be obtained by solving Fick's second law of diffusion on planar surfaces under the boundary condition that the antigen concentration at the solid surface is zero at all times (11). However, a microwell has the geometry of a cylinder with nonplanar surfaces. As a close approximation, we consider only planar surfaces in our calculations. This is valid for the expected diffusion coefficients if $(Dt/r^2) < 0.01$ (r is the inner radius of microwell) in Eq. [4] (12). The concentration of the antigen (B) bound to antibody on the surface is related to the diffusion coefficient (D) and the time (t) by the equation

$$B = 2S[\mathrm{Ag}]_t(Dt/\pi)^{1/2}, \qquad [4]$$

where S is the surface area of a microwell that is covered with liquid and $[\mathrm{Ag}]_t$ is total concentration of antigen based on unit volume. The effective diffusion coefficient D can be computed by iterations for different times with Eq. [4] until the kinetic curve fits the experimentally obtained results (Fig. 4).

Equation [4] has been derived only for three-dimensional mass transfer. However, since we obtained a good fit with experimentally determined data (representing all three processes: three-dimensional, lateral, and rotational diffusion; for details see Part I), we consider the calculated value as the effective diffusion constant. This is in agreement with other investigators' results who determined three-dimensional diffusion to be the major component in mass transfer (13).

Penetration layer thickness (a). To determine the penetration layer thickness, we used the Nernst equation (11). Immediately after the antigen is added to the wells with the immobilized antibody, the association

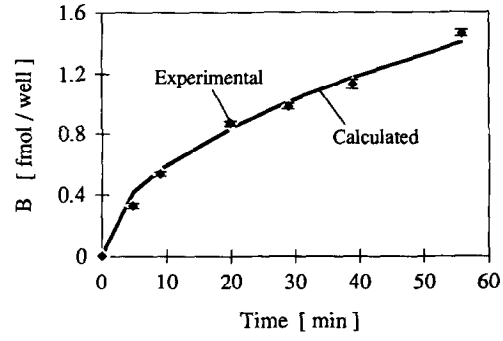

FIG. 4. Determination of the diffusion coefficient, D. Under nonstirring conditions, the progesterone–HRP conjugate was incubated in microwells that contained immobilized antibody. The experimental data were used to obtain a mathematical expression for the diffusion coefficient (Eq. [4]). Averages and standard deviations are shown.

rate of the antigen with the antibody is faster than the molecules can reach the antibody; i.e., the binding reaction is diffusion-controlled (12). Thus, the formation rate of antigen–antibody complex initially reflects the influx of the antigen to the penetration layer from the bulk solution (Part I),

$$d[\text{Ag:Ab}]/dt = (D/a)([\text{Ag}]_b - [\text{Ag}]_s), \quad [5]$$

where [Ag:Ab], $[Ag]_b$, and $[Ag]_s$ are the concentrations of the binding complex, antigen in bulk solution, and antigen at solid surface, respectively. We calculate the initial slope of the kinetic binding curve (reaction rate ($d[Ag:Ab]/dt$) at $t = 0$). Substituting the slope, $[Ag]_b = [Ag]_t$, and $[Ag]_s = 0$ into [5], we obtain [6] as an expression of the penetration thickness (a):

$$a = (D[\text{Ag}]_t)/\{d[\text{Ag:Ab}]/dt\}_{t=0}. \quad [6]$$

The penetration thickness was experimentally determined by Eq. [6] at constant agitation on an orbital shaker.

Determination of Independent Variables for Native Antigen

Unlike labeled antigens, the native antigen does not generate signals that are readily measurable. Therefore, the four variables mentioned above that are required for the calculations of the numerical or analytical solution can only be obtained by indirect methods.

For the example presented here, we have substituted three variables for the native antigen (total concentration of antibody interacting with the native antigen, diffusion coefficient, and penetration layer thickness) by results obtained with an ^{125}I-labeled derivative of progesterone. The molecular dimensions of native progesterone (M_r 315) and the radiolabeled derivative (M_r 730) are close when compared with the progesterone–HRP conjugate (M_r 40,000). Therefore, the deviations for the determination of the diffusion coefficient and the penetration layer thickness are negligible. Likewise, it is assumed that binding of the radiolabeled tracer to the immobilized antibody is similar to the native antigen for the determination of binding sites on the microwells.

It is difficult to determine the reaction kinetic constants (k_{on} and k_{off}) for antigen–antibody binding by means of the radiolabeled tracer because the interaction between this conjugate and the antibody might be affected by the chemical modification of the native antigen (e.g., by bridge group recognition (2,14)). Therefore, we have used indirect methods to obtain the equilibrium binding constant (K_a) and the off-rate constant (k_{off}). The on-rate constant (which cannot be easily determined directly because of lack of signal) can then be calculated from K_a and k_{off} by the relationship: $K_a = k_{on}/k_{off}$.

Equilibrium binding constant (K_a) of native antigen. The equilibrium constant of the native antigen can be derived from a regular dose–response curve obtained with a labeled derivative of the analyte (tracer) (5). To this end, we need a mathematical expression that fits an experimentally obtained dose–response curve. Five equations need to be developed that contain expressions for five different variables, the concentrations of analyte–antibody complex, tracer–antibody complex, free analyte, free tracer, and unoccupied antibody. In three material balance equations (for the analyte, the tracer, and the antibody), two association constants (for the formation of tracer–antibody and for analyte–antibody complex) are substituted. Eventually, an expression for the free antibody concentration $[Ab]_f$, is obtained (superscript * stands for the radiolabeled antigen):

$$1 - ([\text{Ab}]_f/[\text{Ab}]_t)\{1 + K_a^*[\text{Ag}^*]_t/(1 + K_a^*[\text{Ab}]_f) + K_a[\text{Ag}]_t/(1 + K_a[\text{Ab}]_f)\} = 0. \quad [7]$$

The nonlinear equation [7] is difficult to resolve analytically for $[Ab]_f$. Therefore, we used a numerical method (e.g., Newton–Raphson method (15)) to determine $[Ab]_f$ at a given K_a. If $[Ab]_f$ is known, the bound concentration of labeled antigen (B) can now be calculated:

$$B = S[\text{Ag}^*\text{:Ab}] = [\text{Ag}^*]_t\{1 - 1/(1 + K_a^*[\text{Ab}]_f)\}. \quad [8]$$

The calculated ratio B/B_0 (the concentration of the bound tracer in the presence of the native antigen divided by that without the native antigen) at equilibrium is plotted against the concentration of the native antigen (dose–response curve, Fig. 5). The binding constant of the native antigen is then determined by iterative calculations using $[Ab]_f$ from [7] in Eq. [8] for given concentrations of the analyte.

Off-rate constant. By using the radiolabeled antigen, the off-rate constant of the native antigen can be indirectly measured. Under the premise that the on-rate of the radiolabeled antigen is faster than the off-rate of the native antigen (radiolabeled antigen was used in excess to the bound native antigen), the dissociation of the complex between the native antigen and antibody is the rate-limiting step. For our model system, the ratio of the maximum on-rate of ^{125}I-P over the off-rate of the native analyte, i.e., $(k_{on}^*[\text{Ag}]_t^*)/k_{off}$, is greater than 5. This proves that the dissociation rate of the native antigen is slower than the association rate of the radiolabeled antigen, and therefore, the dissociated amount of the native antigen can be determined by measuring the bound labeled antigen without introducing a large error. Ac-

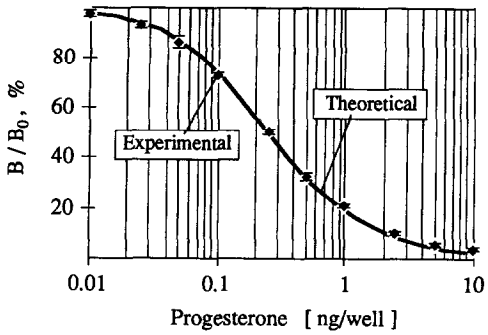

FIG. 5. Experimentally obtained dose–response curve (^{125}I-progesterone derivative as tracer) compared with a mathematically derived curve. The theoretically developed mathematical expression was used to calculate the association constant, K_a, for native progesterone. Averages and standard deviations for the experimental data are shown.

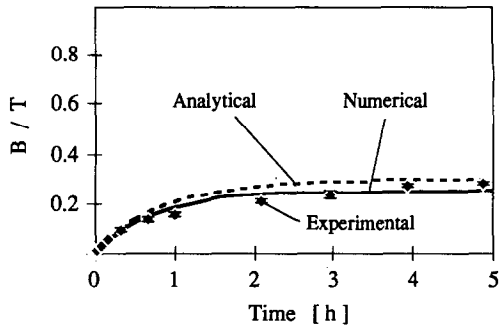

FIG. 6. Kinetic binding curves of progesterone–HRP conjugate to antibody immobilized on a solid matrix. Theoretical calculations by two different methods (analytical and numerical solutions) correlated well with empirical determinations (done in duplicate). Binding of the conjugate to the immobilized antibody is expressed as a ratio of bound over total antigen (B/T). Replicate experimental values did not exceed 6% of the mean for time points after 0.3 h.

cording to Eq. [3], the calculated B/B_0 for the native antigen is plotted against time to determine the off-rate constant for the native antigen.

Comparison between Theoretical Calculations and Experimental Results: Kinetic Binding Patterns of Different Sizes of Antigen

We have developed the mathematical model (Part I) for the binding reaction between antigen and antibody at the liquid–solid interfaces. The independent variables required for the calculations were empirically determined as described above and listed in Table 1. In this section, the kinetic binding curves (plots of B/T vs time) calculated by the two methods (analytical and numerical solutions) are presented together with the experimental results for three different antigen species (progesterone–HRP conjugate, ^{125}I-labeled progesterone, and native progesterone). All experiments shown in this section were performed under stirring conditions.

Kinetic Binding of Progesterone–HRP Conjugate

The kinetic binding curves obtained by theoretical calculations (analytical and numerical solutions) agreed well with experimental data (Fig. 6). The slightly better fit of the experimental data with the numerical solution is of little practical value since all data were so close. In conclusion, both the analytical and the numerical solutions can be used for predicting antigen–antibody binding complex formation.

The agreement of calculated kinetic binding curves with experimentally determined binding over time is encouraging for setting up computer models for the optimal performance of immunosensors. With a minimum of labor intensive, experimentally obtained data, predictions can be made as to the requirements of quality and quantity of components of the analytical system.

It took more than 4 h for the progesterone–HRP conjugate to reach equilibrium at which the on-rate and the off-rate are identical. This was about four times longer than for the two smaller antigens (Figs. 7 and 8). The larger molecule diffuses slower at a given concentration gradient as driving force.

The ratio of bound over total antigen (B/T) at equilibrium is determined by two factors: (a) the equilibrium binding constant between antibody and antigen and (b) the concentration of the reactants. In these experiments (Figs. 6 and 7), we kept the concentrations of enzyme labeled and radiolabeled antigen about constant for easier comparison of the results. With the enzyme tracer, the concentration of binding sites was estimated to be about 5 to 8 $\times$ 10^{-17} mol/mm^2 (Table 1). However, the same batch of wells showed a larger number of binding

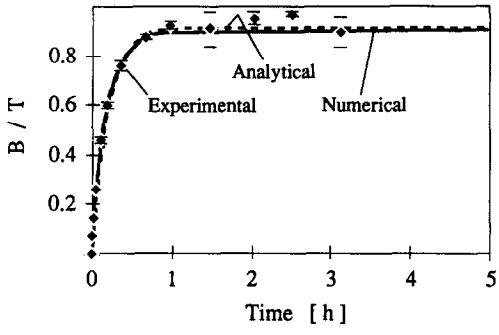

FIG. 7. Kinetic binding curves of an ^{125}I-progesterone derivative to antibody immobilized on a solid matrix. The experimental results and theoretical calculations by two different methods agreed very well, as was seen with the enzyme labeled analog (Fig. 6). Each data point is the mean of duplicate determinations; the replicate values did not exceed 8% of the mean.

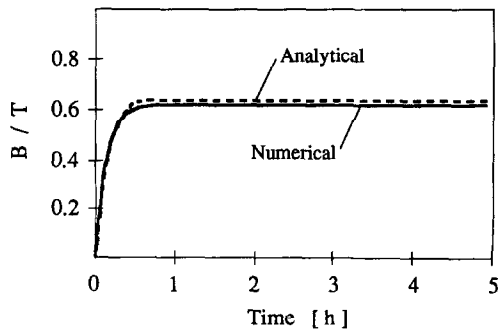

FIG. 8. Kinetic binding curves of native progesterone to antibody immobilized on a solid matrix, calculated by the analytical and numerical solution.

sites if experimentally determined with a radiolabeled derivative as tracer (see below).

Kinetic Binding of ^{125}I-Progesterone

With an ^{125}I-labeled derivative of progesterone as antigen, experimental results for binding over time were very closely reflected by theoretical calculations, when either the numerical or the analytical solution was used (Fig. 7). This is in agreement with the results obtained with the analyte–enzyme conjugate (see above).

Initial binding of the radiolabeled antigen, which has less mass than the enzyme-labeled counterpart, is much faster. According to our calculations (Eq. [4]), the diffusion coefficient of the smaller antigen was about 12 times higher (Table 1).

The ratio of bound over total antigen is higher for the radiolabeled derivative than for the enzyme conjugate. Both antigens have a binding constant with the antibody that is not much different (10^{10} M^{-1} from Scatchard analysis). However, the effective concentration of binding sites measured with the radiolabeled tracer on the same batch of microwells was about 15 times higher than measured with the enzyme tracer (Table 1). There can be two reasons for this: (a) the enzyme conjugate can only utilize a limited number of antibody binding sites because of the large size of the enzyme, and/or (b) a nonhomogeneous population of binding sites exists on the surface. Scatchard analyses do not support the second option, although technical limitations might exist. At high B/F ratios, measurements with the enzyme tracer become very inaccurate because color development sets in very rapidly. We are currently further investigating both working hypotheses.

Kinetic Binding of Native Progesterone

As mentioned previously, the native antigen does not provide a measurable signal, so the experimental determination of kinetic binding curves is difficult. The theoretical models are of particular value here (Fig. 8). However, to execute the calculations, certain constants need to be entered into the computer programs. As mentioned above, we described the derivation of k_{off} and k_{on}, the off- and on-rate constants for binding of native progesterone to the antibody. We have substituted the constants for the penetration layer thickness, the number of binding sites on the solid matrix, and the diffusion coefficient, using values obtained from the radiolabeled tracer. The differences of these constants between the native antigen and the radiolabeled tracer are negligible. Even for the determination of the diffusion coefficient, doubling the size of the molecules does not substantially change the diffusion rate (e.g., the diffusion coefficient of native progesterone is 1.5 times higher than that of the ^{125}I-progesterone derivative, but 12 times higher than the enzyme–progesterone conjugate).

Binding of native progesterone at equilibrium was lower than for the radiolabeled derivative because the binding constant is lower (3×10^9 M^{-1}).

In an enzyme immunoassay, it is the competition between the native and labeled antigens that determines the formation of the antigen–antibody complex over time (e.g., a combination of the curves shown in Figs. 6 and 8). We analyze this situation below.

Dose–Response Curves with an Enzyme Tracer at Nonequilibrium and Equilibrium Conditions

In competitive immunoassays, two antigens are recognized by the antibody: the analyte–enzyme conjugate and the native antigen in the sample. The two antigens

TABLE 1

Experimentally Determined Parameters for Labeled and Native Antigens

	P-HRP	^{125}I-P	Native P	Dimension
Molecular weight	40,000	730	315	—
Ab surface density[a]				
1[b]	7.7×10^{-17}	1.3×10^{-15}	—	mol mm^{-2}
2[c]	5.0×10^{-17}	7.3×10^{-16}	—	mol mm^{-2}
On-rate constant[d]	3.2×10^{12}	2.7×10^{12}	4.2×10^{12}	mm^3 mol^{-1} s^{-1}
Off-rate constant[d]	4.5×10^{-4}	2.5×10^{-4}	1.4×10^{-3}	s^{-1}
Diffusion coefficient	3.0×10^{-5}	3.7×10^{-4}	—	mm^2 s^{-1}
Penetration layer thickness	8.1×10^{-2}	9.2×10^{-2}	—	mm

[a] The antibody surface density (mol mm^{-2}) represents the amount of P-Ab (BQ.1) immobilized per unit surface area of microwells.

[b] Values obtained by coating with 200 μl per well of an antibody solution of 5 μg/ml. These wells were used for the determination of the independent variables (see text) and for the kinetic binding curves.

[c] Values obtained by coating with 200 μl per well of an antibody solution of 2.5 μg/ml. These wells were used for dose–response curves.

[d] The rate constants were determined for P-Ab (BQ.1).

compete for the same binding sites on the antibody but the smaller antigen reaches the antibody on the surface faster so that initial competition between the two antigens is different than at equilibrium. This is shown in Fig. 9.

For the construction of dose–response curves, we coated the antibody at two times lower concentration (2.5 μg/ml, see Table 1) to the surface of microwells compared to the wells used for the determination of the independent variables (surface density, on- and off-rate constants, effective diffusion coefficient, and penetration layer thickness) and the kinetic binding curves. This resulted in a lower surface density of the antibody and, therefore, in a higher sensitivity of the analytical system while the other variables were not affected.

The calculations for kinetic binding curves in this section were based on the mathematical model developed in Part I for the binding of a single antigen to the antibody. We extended the equations from Part I to two antigens to reflect the situation in a competitive binding assay. We obtained one equation for diffusion and one for antigen–antibody complex formation for each antigen (progesterone and progesterone–HRP conjugate). We theoretically calculated binding curves by the numerical method after combining the material balance equations for each antigen and for the antibody.

In the absence of native progesterone (Fig. 9, B_0/T'), the enzyme–progesterone conjugate diffuses to the surface and forms the antigen–antibody complex until equilibrium is asymptotically reached where the on-rate and the off-rate are equal; i.e., the reaction is no longer diffusion controlled. The ratio of B/T' is smaller in the presence of native progesterone ($B_{0.025}/T'$; bound enzyme tracer measured in the presence of 0.025 ng/well of progesterone). Formation of the antigen–antibody complex with native progesterone under these conditions (Fig. 9, dashed curve; $P_{0.025}/T'$) is much faster than

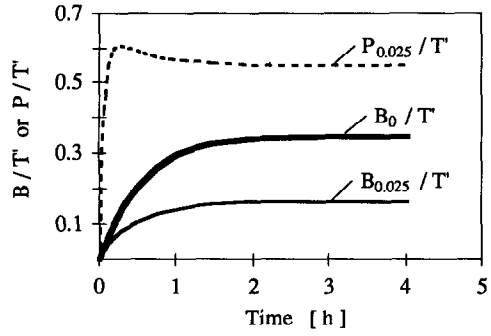

FIG. 9. Theoretical kinetic binding curves. The bound antigen (enzyme tracer: B; progesterone: P) is expressed as a ratio of total amount of immobilized antibody (T'). The subscripts are: B_0 bound enzyme tracer in the absence of native progesterone; $B_{0.025}$ bound enzyme tracer in the presence of 0.025 ng/well of progesterone; and $P_{0.025}$ binding of 0.025 ng/well of free progesterone over time.

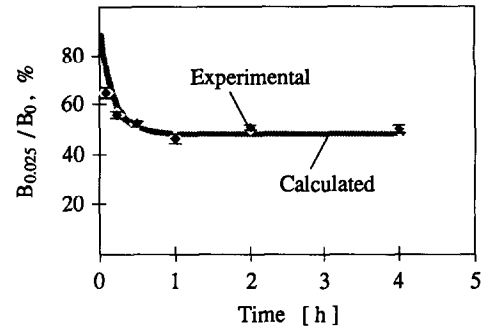

FIG. 10. The ratio $B_{0.025}/B_0$ (see Fig. 9) over time. After 30 min, equilibrium is reached at 50% binding of the enzyme–progesterone tracer. Experimentally obtained results correlate well with the calculated kinetic curve. Each data point is the mean of duplicate measurements; the replicate values did not exceed 6% of the mean.

with the enzyme–progesterone conjugate. It peaks at about 15 min to decrease somewhat thereafter and remain constant. The initial peak comes from higher progesterone–antibody complex formation due to lack of competing progesterone–HRP conjugate that diffuses slower. After a sufficient amount of the enzyme conjugate reaches the immobilized antibody, some of the progesterone molecules are displaced by conjugate, and equilibrium is eventually reached. In the absence of progesterone-enzyme conjugate, the dashed line in Fig. 9 can be compared with the binding curve in Fig. 8.

It is the interaction between these kinetic curves that determines the performance of immunosensors under nonequilibrium conditions in competitive immunoassays with antigens of different size, e.g., if the analyte is substantially smaller than the analyte–enzyme conjugate.

In competitive immunoassays, the analyte competes with the analyte–enzyme conjugate (tracer) for antibody binding sites. Traditionally, this relationship is expressed as the ratio of tracer bound (B) at different analyte concentrations over tracer bound in the absence of analyte (B_0). As mentioned above, the competition between the two antigen species is time dependent. If at a constant concentration of native antigen (e.g., 0.025 ng/well of progesterone, Fig. 10) the ratio B/B_0 is experimentally determined, it can be shown that under the conditions of these experiments, this ratio becomes constant shortly after 30 min.

This experiment provided a noteworthy result. As we have mentioned earlier, an identical preparation of antibody immobilized to the surface reveals about 15 times more binding sites if determined by Scatchard analysis with the smaller radiolabeled tracer compared to the enzyme–progesterone conjugate. The Scatchard plots follow a linear regression with good correlation for both antigens and we have not yet found any indication for a heterogeneous population of binding sites. Presumably,

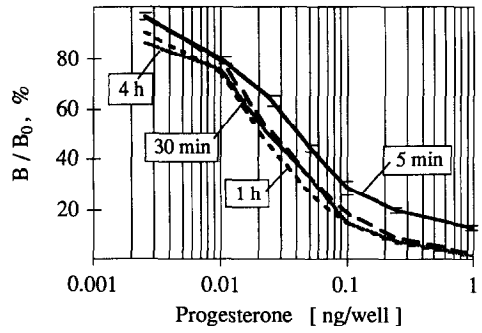

FIG. 11. Dose–response curves of progesterone with a progesterone–HRP conjugate as signal generator and an immobilized monoclonal antibody at different incubation times at stirring conditions. At a short incubation time when the antigen–antibody complex formation is diffusion controlled (5 min), a less sensitive dose–response curve is obtained. For the 5-min curve, the range of duplicate estimations is shown.

the large size of the analyte–enzyme conjugate prohibits its access to all available binding sites. If the native antigen displaces the enzyme–progesterone conjugate as shown in Fig. 10, the native progesterone should have all the binding sites available. However, the theoretical model correlates with the experimental results only if the number of binding sites available for the enzyme conjugate are entered. This strongly suggests that the analyte–enzyme conjugate is preferentially dissociated before other binding sites are occupied by the native progesterone. The mechanism of action of this process is the subject of further investigations.

The time-dependent shift of the ratio B/B_0 shows that measurements under nonequilibrium conditions with immunosensors that are not simultaneously calibrated with standards need to be timed very precisely. However, under equilibrium conditions, timing of the incubation period is less important for accurate measurements.

Finally, we have investigated the effect of incubation time on the performance of dose–response curves. It becomes clear from the experiments shown in Fig. 10 that the "signal yield" is higher at longer incubation times; i.e., 0.025 ng/well of progesterone can displace about 50% of the enzyme tracer after 30 min of incubation while only about 30% is displaced after 5 min (70% of the tracer is bound). Therefore, dose–response curves are less sensitive if performed at shorter incubation times (Fig. 11). If we define the sensitivity as the amount of analyte that displaces 50% of the tracer, about twice as much progesterone is required for 50% displacement after 5 min of incubation as compared with 30 min and longer (i.e., at equilibrium). As expected from results shown in Fig. 10, dose–response curves at incubation times longer than 30 min are not significantly different. The differences shown in Fig. 11 reflect experimental variations.

These studies have shown that quantitative measurements with immunosensors can be made after a few minutes of incubation. It is also notable that the progesterone–HRP conjugate requires 3 to 4 h to reach equilibrium for the formation of antigen–antibody binding complex (Fig. 6) but dose–response curves in a competitive binding assay with the same enzyme conjugate as tracer do not substantially change anymore after about 30 min.

It should be emphasized that the quantitative relationships shown in this section are idiosyncratic for this particular analytical system. In particular, the binding constants between the antibody and the two antigens (analyte and the analyte–enzyme conjugate) can substantially affect the dose–response curves at different incubation times. Therefore, for other applications, each antigen–antibody combination needs to be separately investigated.

As we have mentioned earlier, all experiments described in this publication were carried out under stirring conditions, if not specified otherwise. It is of practical value to know the difference of antigen–antibody formation between stirring and nonstirring conditions. As we have shown, diffusion can substantially affect quantitative measurements under nonequilibrium conditions. However, is agitation necessary under equilibrium conditions?

Since the diffusion rate is partially a function of volume, it is desirable to operate an immunosensor with small reaction volumes. The volume for three-dimensional diffusion can be reduced by agitation, but a penetration layer still remains. With 200 μl of liquid in the microwells as used in these experiments, reducing the volume for three-dimensional diffusion by agitation did not contribute substantially to increased diffusion rates. We found little difference in the dose–response curves whether the wells were agitated or not (Fig. 12).

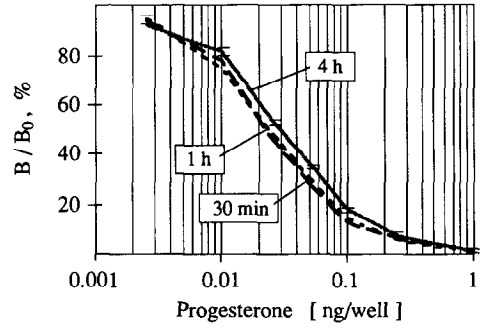

FIG. 12. Dose–response curves at different incubation times under nonstirring conditions. If the reaction is no longer diffusion controlled, the sensitivity of dose–response curves is similar to those at stirring conditions (see Fig. 11). For the 4-h curve, the range of duplicate estimations is shown.

For 50% inhibition of the enzyme tracer at stirring conditions, 21 to 25 pg/well of progesterone was required at equilibrium (i.e., incubation times >30 min) compared to 25 to 29 pg/well under nonstirring conditions.

ACKNOWLEDGMENTS

We are indebted to Drs. Leonidas G. Bachas, Richard H. Smith, and Paul A. Craig for critical discussions. This work was supported by the Army Research Office (246655-LS) and a grant from the National Institutes of Health (NICHHD, HD22316).

REFERENCES

1. Paek, S.-H., and Schramm, W. (1991) *Anal. Biochem.* **196**.
2. Schramm, W., Yang, T., and Midgley, A. R. (1987) *Clin. Chem.* **33,** 1331–1337.
3. Sanderson, C. J., and Wilson, D. V. (1971) *Immunology* **20,** 1061–1065.
4. Scatchard, G. (1949) *Ann. N.Y. Acad. Sci.* **51,** 660–672.
5. Munson, P. J. (1983) *in* Methods in Enzymology (Langone, J. J., and Van Vunakis, H., Eds.), Vol. 92, pp. 543–576, Academic Press, San Diego.
6. Zettner, A. (1973) *Clin. Chem.* **19,** 699–705.
7. Schramm, W., Yang, T., and Midgley, A. R. (1987) *Clin. Chem.* **33,** 1338–1342.
8. Bos, E. S., van der Doelen, A. A., van Rooy, N., and Schuurs, A. H. (1981) *J. Immunoassay* **2,** 187–204.
9. Smith, T. W., and Skubitz, K. M. (1975) *Biochemistry* **14,** 1496–1502.
10. Schonbrunn, A., and Tashijan, A. H. (1978) *J. Biol. Chem.* **253,** 6473–6483.
11. Trurnit, H. J. (1954) *Arch. Biochem.* **51,** 176–199.
12. Stenberg, M., Werthen, M., Theander, S., and Nygren, H. (1988) *J. Immunol. Methods* **112,** 23–29.
13. Wiegel, F. W., and DeLisi, C. (1982) *Am. J. Physiol.* **243,** R475–R479.
14. Hosoda, H., Kawamura, N., and Nambara, T. (1981) *Chem. Pharm. Bull* **29,** 1969–1974.
15. Carnahan, B., Luther, H. A., and Wilkes, J. O. (1969) Applied Numerical Methods, pp. 319–329, Wiley, New York.